The Phanerozoic diversification of silica-cycling testate amoebae and its possible links to changes in terrestrial ecosystems

Daniel J.G. Lahr[1], Tanja Bosak[2], Enrique Lara[3] and Edward A.D. Mitchell[3,4]

[1] Department of Zoology, Institute of Biosciences, University of São Paulo, Rua do Matão, São Paulo, Brazil
[2] Department of Earth, Atmospheric and Planetary Sciences, Massachussetts Institute of Technology, Cambridge, MA, USA
[3] Laboratory of Soil Biology, University of Neuchatel, Neuchatel, Switzerland
[4] Jardin Botanique de Neuchâtel, Neuchatel, Switzerland

ABSTRACT

The terrestrial cycling of Si is thought to have a large influence on the terrestrial and marine primary production, as well as the coupled biogeochemical cycles of Si and C. Biomineralization of silica is widespread among terrestrial eukaryotes such as plants, soil diatoms, freshwater sponges, silicifying flagellates and testate amoebae. Two major groups of testate (shelled) amoebae, arcellinids and euglyphids, produce their own silica particles to construct shells. The two are unrelated phylogenetically and acquired biomineralizing capabilities independently. Hyalosphenids, a group within arcellinids, are predators of euglyphids. We demonstrate that hyalosphenids can construct shells using silica scales mineralized by the euglyphids. Parsimony analyses of the current hyalosphenid phylogeny indicate that the ability to "steal" euglyphid scales is most likely ancestral in hyalosphenids, implying that euglyphids should be older than hyalosphenids. However, exactly when euglyphids arose is uncertain. Current fossil record contains unambiguous euglyphid fossils that are as old as 50 million years, but older fossils are scarce and difficult to interpret. Poor taxon sampling of euglyphids has also prevented the development of molecular clocks. Here, we present a novel molecular clock reconstruction for arcellinids and consider the uncertainties due to various previously used calibration points. The new molecular clock puts the origin of hyalosphenids in the early Carboniferous (~370 mya). Notably, this estimate coincides with the widespread colonization of land by Si-accumulating plants, suggesting possible links between the evolution of Arcellinid testate amoebae and the expansion of terrestrial habitats rich in organic matter and bioavailable Si.

Subjects Biochemistry, Biodiversity, Evolutionary Studies, Microbiology, Paleontology
Keywords Amoebozoa, Evolution of eukaryotes, Conquer of terrestrial environment, Molecular clocks, Testate amoebae, Silica cycle, Coupled carbon and silica cycles, Vase shaped microfossils, Ancestral state reconstruction

Submitted 29 May 2015
Accepted 19 August 2015
Published 8 September 2015

Corresponding author
Daniel J.G. Lahr, dlahr@ib.usp.br

Academic editor
Kenneth De Baets

Additional Information and Declarations can be found on page 14

DOI **10.7717/peerj.1234**

INTRODUCTION

Si is a major rock-forming element with a cycle that influences the growth of primary producers and carbon burial in the oceans (*Sarmiento, 2013*). Over geological time scales, the biogeochemical cycles of carbon and silica are linked through the weathering of continents, which dissolves Si from rocks and delivers it to the oceans (*Wilkinson & Mitchell, 2010*). On shorter time scales, Si cycles vigorously in soils and forms a soil pool that is 2–3 orders of magnitude larger than the Si pool in living terrestrial biomass (*Cornelis et al., 2011*). Thus, plant-microbe-mineral interactions that control this sizeable pool of soil Si ultimately control the availability of dissolved Si and the delivery of Si to the oceans (*Conley, 2002*). Plants are thought to be the major contributors to the terrestrial cycling of Si because they can promote the weathering of rocks, accumulate Si from the soil solution and biomineralize amorphous Si in the form of phytoliths (*Alexandre et al., 1997*; *Cornelis et al., 2011*). Phytoliths released from dead plant matter can form a pool with a lower turnover rate relative to other forms of biogenic silica (*Alexandre et al., 1997*). This pool comprises more than 90% of biogenic Si delivered to rivers (*Cary et al., 2005*) and is the main source of reactive Si in soils. Research in the past three decades has revealed much about the role of plant-derived biogenic Si in the terrestrial cycling of Si (*Conley, 2002*). In contrast, the contribution and the long term history of Si-biomineralizing microbial groups in terrestrial ecosystems are less well understood (*Wilkinson & Mitchell, 2010*). Many microbial eukaryotes use silica to build external and internal skeletons, and have molecular mechanisms for Si uptake. Up to 77 genes regulated by silicic acid in the diatom *Phaeodactylum tricornutum* have orthologs in the genomes of other eukaryotes, including Opisthokonts, Viridiplantae and other "Chromalveolates" (*Sapriel et al., 2009*); see also Fig. 1. The genes implicated in silica metabolism may have been exchanged among eukaryotic clades through lateral gene transfer, as demonstrated for choanoflagellates and diatoms (*Marron et al., 2013*). In terrestrial systems, testate amoebae (i.e., amoebae that construct shells) are among the most abundant and conspicuous organisms that use silica. The existing studies show that: (1) testate amoebae can contribute up to 10% of biogenic silica in some tropical soils and rivers (*Cary et al., 2005*); and (2) the annual incorporation of Si by testate amoebae can in some cases match the amounts of Si released by plant phytoliths (*Aoki, Hoshino & Matsubara, 2007*; *Wilkinson, 2008*; *Sommer et al., 2012*; *Puppe et al., 2014*). These observations, as well as the long evolutionary history of testate amoebae (*Lahr, Grant & Katz, 2013*), suggest a role for testate amoebae in the terrestrial silica cycle and motivate this study.

There are several groups of unrelated testate amoebae. The two most prevalent and abundant in terrestrial environments are the euglyphid and the arcellinid testate amoebae. Both inhabit the same environments—bodies of fresh water, soils, peatlands and other humid microhabitats—and have approximately the same sizes, with the majority of species being between 30–300 μm long or wide. However, the two groups are vastly divergent genetically and historically. Euglyphids include about 800 species and are in the super group Rhizaria (Fig. 1). These organisms produce thin, pointed, non-anastomosed pseudopods and almost all extant lineages in the group are silica biomineralizers.

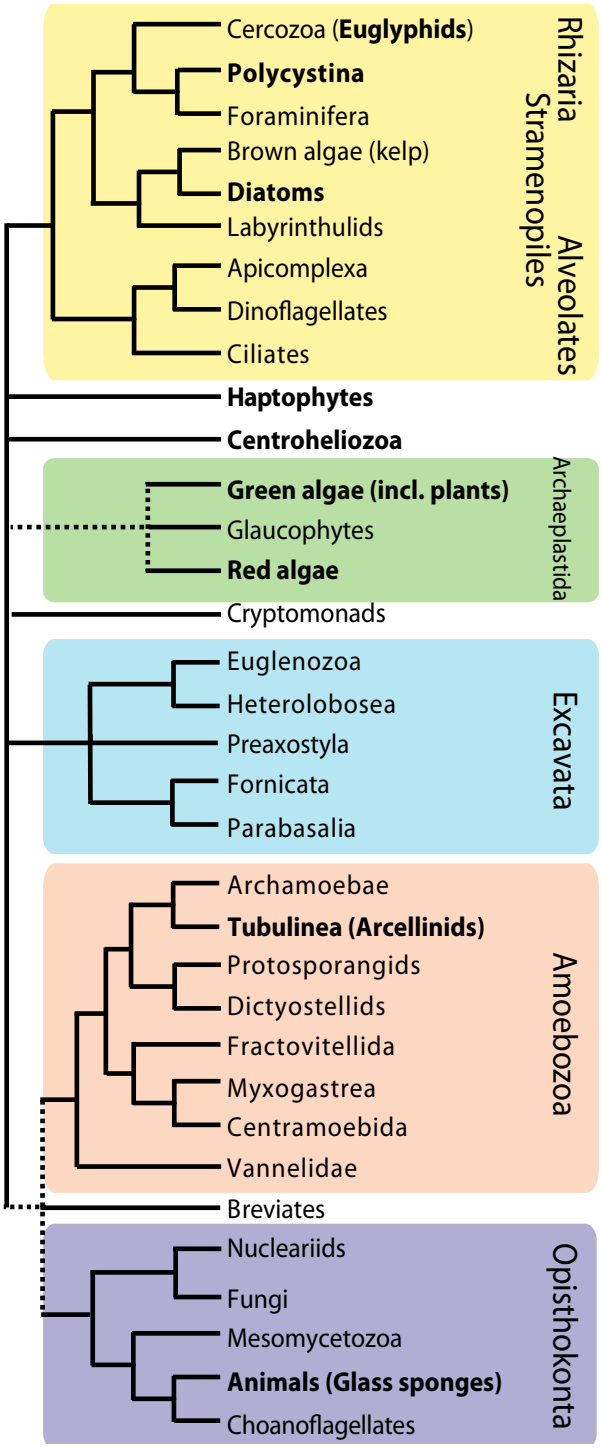

Figure 1 A simplified tree of eukaryotes indicating that biomineralization is a convergent feature. The main supergroups are indicated by the different colors and the lineages in bold contain biomineralizers. Backbone of tree is based on relationships in *Katz (2012)*, dotted lines represent uncertainty.

Thus, biomineralization is likely ancestral in the group. Owing to the preservation of siliceous shells, euglyphids have a reliable fossil record that goes back at least 30–50 million years (*Foissner & Schiller, 2001*; *Barber, Siver & Karis, 2013*). The arcellinid testate amoebae encompass about 2,000 species and are in the super group Amoebozoa (Fig. 1). These amoebae produce rounded, blunt pseudopods and have a great diversity of shell compositions—organic, agglutinated and biomineralized. The fossil record of arcellinids is much older than that of euglyphids, and there is consensus that some vase shaped microfossils dating back to the Neoproterozoic (ca. 750 mya) belong to the arcellinids (*Porter & Knoll, 2000*; *Bosak et al., 2011*; *Lahr, Grant & Katz, 2013*; *Strauss et al., 2014*).

Biomineralization of silica in testate amoebae occurs in many different ways. The shell is always constructed shortly before cell division: a new shell is produced through the aperture of the older shell. After cell division, one daughter cell stays in the old shell and the other daughter cell inherits the new shell (*Hedley & Ogden, 1974*). Most euglyphids produce silica scales in the cytoplasm, presumably taking up dissolved Si and depositing it as amorphous silica *via* silica deposition vesicles (*Hedley & Ogden, 1974*; *Anderson, 1994*; *Gröger, Lutz & Brunner, 2008*). The scales, which are typically shorter than 10 μm and thinner than 2 μm, are then used as building blocks to construct the shell. The specific literature refers to these types of building blocks produced by testate amoebae as *idiosomes*. A small number of arcellinids use a similar strategy—*Lesquereusia*, *Netzelia*, and especially *Quadrulella* (Fig. 2A) are three genera known to produce silica idiosomes (*Anderson, 1987*; *Anderson, 1989*; *Anderson, 1994*; *Meisterfeld, 2002*). *Netzelia* is able to precipitate idiosomes, but is also known to deposit silica around ingested particles, including starch and various minerals, and then use these particles to build the daughter shell (*Anderson, 1987*; *Anderson, 1989*). *Quadrulella*, on the other hand, produces its shell entirely of square siliceous idiosomes. Many arcellinids use siliceous particles and mineral grains scavenged from the environment as unmodified building blocks named *xenosomes* (*Difflugia* (Fig. 2B) and *Heleopera* are well-known examples (*Meisterfeld, 2002*; *Châtelet, Noiriel & Delaine, 2013*)). Others are able to lightly modify siliceous particles either by dissolution or deposition (e.g., *Nebela* (Fig. 2C) and related genera (*Padaungiella, Argynnia* (Fig. 2D)), as well as the *insertae sedis Lesquereusia* (*Anderson, 1987*; *Anderson, 1989*).

Both classical and modern studies report the usage of euglyphid scales by arcellinid amoebae of the Hyalospheniidae family (*Leidy, 1879*; *Penard, 1902*; *Deflandre, 1936*; *Douglas & Smol, 2001*; *Meisterfeld, 2002*). These amoebae reportedly obtain silica plates by preying on euglyphids, and then use the stolen scales to build the shell (*Deflandre, 1936*)—a phenomenon we name *kleptosquamy* (Fig. 3). Here, we record several stages of this phenomenon in *Padaungiella lageniformis* that preys upon *Euglypha* sp. Next, we ask whether *kleptosquamy* is ancestral in the hyalosphenid testate amoebae and use this to determine the order in which hyalosphenids and euglyphids emerged. To better time the rise of biomineralization in hyalosphenids, we also provide a novel molecular clock reconstruction of the arcellinids. Finally, we discuss the implications of the revised molecular clock in light of broader evolutionary and biogeochemical trends.

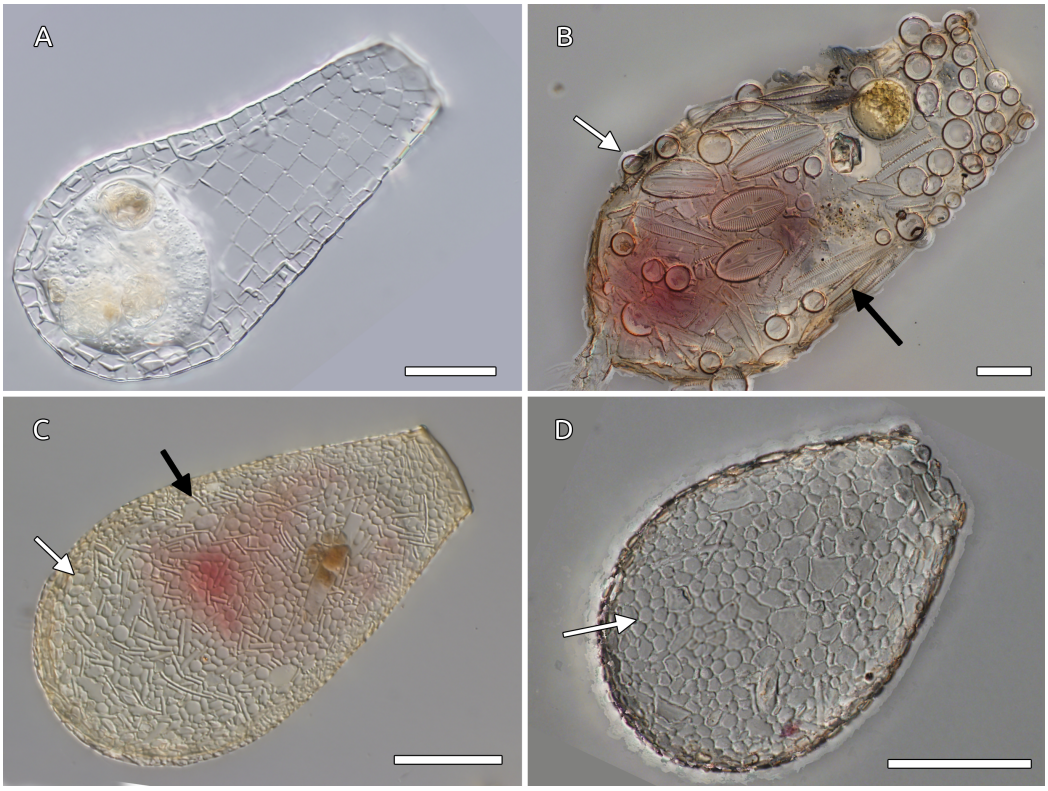

Figure 2 Examples of arcellinids shell composition. (A) *Quadrulella subcarinata* Gautier-Lièvre, 1957 constructs the shell using square particles of amorphous Si that are endogenously produced from dissolved silica (idiosomes). Specimen from *Sphagnum* collected in Welgevonden Game Park, Limpopo province, South Africa. (B) *Difflugia acuminata* Ehrenberg builds its shell from agglutinated diverse particles, in this case, the organism used both centric (white arrow) and pennate (black arrow) diatom shells, along with other smaller particles. (C) *Nebela marginata* Penard uses a mixture of particles with some additional biological silica deposition, such as scales scavenged from euglyphids (oval and circular plates as the one indicated by the white arrow), and pennate diatoms (black arrow). (D) *Argynnia dentistoma*, this specimen has used a mixture of flat environmental mineral particles and rounded euglyphid scales to construct the shell. (B–D): Specimens from Eugene Penard's collection, deposited at the Natural Museum of Geneva; photos taken by Thierry Arnet–Wikimedia document. Scale bars 30 μm.

MATERIAL AND METHODS

Microscopical observations

Samples of *Sphagnum* sp. were collected in *Les Pontins* peat bog in Canton Bern, Switzerland (47°7′39.11″N; 6°59′27.35″E). Microscopic observations were made using an Utermöhl chamber (Cat #435025; HydroBios, Kiel, Germany) on an Olympus IX81 inverted microscope equipped with oil immersion Differential Interference Contrast optics (20×–40×–60×–100×). All images were recorded by an Olympus DP-71 camera.

Ancestral state reconstructions

We have performed ancestral state reconstructions on the topologies from molecular reconstructions of two recently published phylogenies (*Kosakyan et al., 2012*; *Oliverio et al., 2014*). Each reconstruction is based on a distinct set of molecular data (Cox1 and

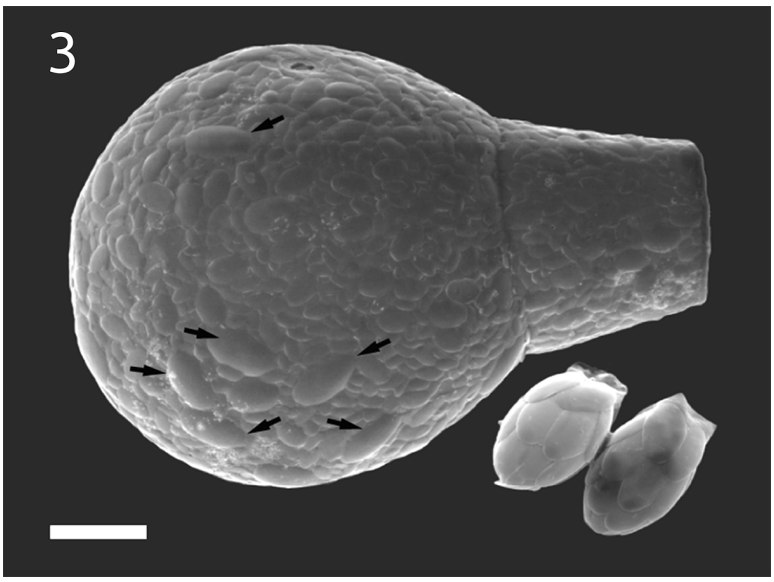

Figure 3 An example of *kleptosquamy* in the arcellinid *Apodera vas* (larger shell), obtained from predation upon the euglyphid *Sphenoderia valdiviana* (two smaller individuals). The two species occur together in *Sphagnum magellanicum* mosses around Laguna Esmeralda, in Argentinian Tierra del Fuego. The larger scales (arrows) in the test of *A. vas* can clearly be matched to the ones produced by *S. valdiviana*.

SSU rDNA respectively). Ancestral state reconstruction was performed in the program Mesquite (*Maddison & Maddison, 2007*) using parsimony as an optimality criterion, for the single character *kleptosquamy*, with possible states present, absent or unknown.

Molecular clock reconstructions

Molecular clock reconstructions (MCR) were performed using PhyloBayes 3.3 (*Lartillot, Lepage & Blanquart, 2009*). We used the final tree and alignment for SSU rDNA small subunit ribosomal gene published by *Lahr, Grant & Katz (2013)* as a tree onto which we calculated divergence times. Calibration points were the 6 opisthokont fossils also used by *Parfrey et al. (2011)*, whereas the Arcellinida calibration point is based on the fossil *Paleoarcella athanata* (type specimen HUPC #62988), described in *Porter, Meisterfeld & Knoll (2003)*. The dating of sedimentary rock for this fossil was an ash bed 2 m above the fossils, calculated by U–Pb zircon chronology (*Karlstrom et al., 2000*) (Table 1). The opisthokont fossils used by *Parfrey et al. (2011)* are congruent with those proposed and justified for animals by *Benton et al. (2015)*. With additional data present in the current tree, it was possible to use the Chuar group fossils as a calibration point for the actual last common ancestor of arcellinids (*Porter & Knoll, 2000*), rather than the divergence between arcellinids and other naked amoebae, as in Parfrey and colleagues (*2011*). One alternative run was also generated incorporating the three additional Meso- and Cenozoic fossils as calibration points within the Arcellinida, as suggested by *Fiz-Palacios, Leander & Heger (2014)*: origin of the *Centropyxis* genus (termed "node B" in *Fiz-Palacios, Leander & Heger (2014)*) was set to the split between *Hyalosphenia papilio* and *Arcella hemisphaerica*, with

Table 1 Summary of calibration points used of molecular clock reconstructions. Dates are in millions of years.

Clade	Fossil	Taxa used for delimitation	Max date	Min date
Amniota	*Westlothiana*	*Gallus gallus* and *Homo sapiens*	400	328.3
Ascomycetes	*Paleopyrenomycetes*	*S.s pombe* and *P. chrysosporium*	1,000	400
Endopterygota	Mecoptera	*A. mellifera* and *D. melanogaster*	350	284.4
Animals	sponge biomarkers	*O. carmella* and *C. capitata*	3,000	632
Bilateria	*Kimberella*	*B. floridae* and *C. capitata*	630	555
Vertebrates	*Haikouichthys*	*B. floridae* and *H. sapiens*	555	520
Arcellinida	*Paleoarcella*	*A. hemisphaerica* and *H. sphagni*	3,000	736

lower and upper bounds at 736–220 mya, origin of hyalosphenids ("node C") was set to the split between *Padaungiella lageniformis* and *Hyalosphenia elegans* with soft bounds at 736–100 mya; origin of genus *Arcella* ("node D"), calibrated the clade containing *A. hemisphaerica* and *A. vulgaris* WP with soft bounds at 105–100 mya. We did not include the fourth calibration point suggested by Fiz-Palacios and colleagues (*Lesquereusia–Difflugia* divergence) because the *Lesquereusia* SSU rDNA is not available. Fortunately, Fiz-Palacios and colleagues (*2014*) have tested their dataset for sensitivity to this particular calibration point and have determined that its inclusion does not significantly modify the final result. We have performed MCRs by running two independent chains with a burn-in factor of 100 until the effective size of samples was above 50 and the maximum discrepancy between chains was below 0.3. These parameters are suggested as values for an "acceptable run" by the PhyloBayes manual. We used soft constraints on the calibration dates to account for uncertainty in the fossil dates as advocated by several researchers (e.g., *Donoghue & Benton, 2007*; *Parfrey et al., 2011*). The use of soft constraints requires a model of birth–death for the prior on divergence times. We performed reconstructions using both the GTR and the CAT-GTR models for nucleotide substitutions. We have performed MCR using three distinct models for rate distributions: two auto correlated models (CIR and lognormal) as well as the uncorrelated gamma multipliers model. We performed comparisons for model fit by computing Bayes Factors by thermodynamic integration under the normal approximation, as discussed in Phylobayes 3.3 manual, and recommended in *Lartillot & Philippe (2006)*. In order to do so, a variance–covariance matrix was obtained using the program *estbranches* (part of *multdivtime* package (*Thorne & Kishino, 2003*)), with input parameters calculated in *baseml* (part of the PAML package (*Yang, 2007*)), following instructions by *Rutschmann (2005)*.

RESULTS

Microscopical observations

An individual *Padaungiella lageniformis* was isolated while preying upon a specimen of *Euglypha* sp. The *Euglypha* cytoplasm had been almost completely ingested at the stage of isolation (Figs. 4A–4C). We observed the *P. lageniformis* removing and ingesting siliceous

plates from the prey organism's shell for around 10 min (Fig. 4D). Immediately afterwards, the individual deposited siliceous plates in the inner part of the "neck" of its shell, parallel to the aperture (Fig. 4E) and moved large cytoplasmic debris in the same direction (Figs. 4E and 4F). The organism was constructing a plug in the aperture, which became visible at the end of this activity that lasted for approximately one hour. There was no indication that any of the plates were dissolved in the cytoplasm: all previously ingested plates were kept intact and moved towards the aperture. After one hour, the amoeba added multiple additional layers to the previously laid down barrier (Figs. 4G–4I). Though the scales formed most of the barrier, other types of debris were added as well. After about two hours of actively plugging the aperture, the amoeba encysted, presumably with digestive function (Figs. 4J and 4K). The amoeba remained encysted for at least two more hours. Resumed observations approximately 12 h later revealed that the amoeba had emerged from the digestive cyst and re-ingested all siliceous plates (Fig. 4L). However, the organism had discarded the yellowish-brown types of debris (Fig. 4L). The siliceous plates did not appear to be separated from any other cytoplasmic structures by membranes. Many gathered around the nucleus at times. Two days after the initial ingestion, the amoeba went into a second resting cyst (it is relevant to note that the amoeba was maintained in an environmental sample and had access to ample food items), where it remained for over 24 h, but did not exhibit other relevant changes. We discontinued observations approximately 80 h after initial observation (4 days).

Ancestrality of kleptosquamy

Observations of kleptosquamy and the associated behavioral attitudes enable evolutionary interpretations in other closely related hyalosphenid testate amoebae. The conspicuous plug made of scales created by *Padaungiella*, as well as the presence of modified euglyphid scales in the shell is observed in most other hyalosphenids, including the genera: *Apodera, Certesella* (*Meisterfeld, 2002*), *Porosia* (Fig. 5A), and finally *Nebela* (Fig. 5B). One other genus has shells that contain small, possibly siliceous scales with undetermined origin: *Physochila* and *Argynnia* (Fig. 2D, (*Vucetich, 1974*)) were shown not to be closely related to hyalosphenids (*Gomaa et al., 2012*). Considering the most current molecular data available, *Padaungiella* is a basal lineage (*Lara et al., 2008*; *Heger et al., 2011*; *Gomaa et al., 2012*; *Kosakyan et al., 2012*; *Lahr, Grant & Katz, 2013*). Other four genera (*Apodera, Certesella, Porosia, Nebela*) are able to re-use scales obtained from euglyphids and three others (*Quadrulella*, *Hyalosphenia* and *Alocodera*) do not. We have performed a parsimony based ancestral reconstruction of character states in both topologies available (based on mitochondrial and nuclear genes, Fig. 6). Under any of the two scenarios scenario, kleptosquamy appears in the ancestral hyalosphenid, and is lost twice: once in the genus *Quadrulella*, which biomineralizes its own silica scales and once in *Hyalosphenia*, which builds entirely proteinaceous scales without mineral parts. In the scenario of *Oliverio et al. (2014)*, kleptosquamy is lost 3 times because the genus *Hyalosphenia* is not monophyletic. The non-monophyly of *Hyalosphenia* has no effect on the ancestral character state for hyalosphenids as a whole (Fig. 6).

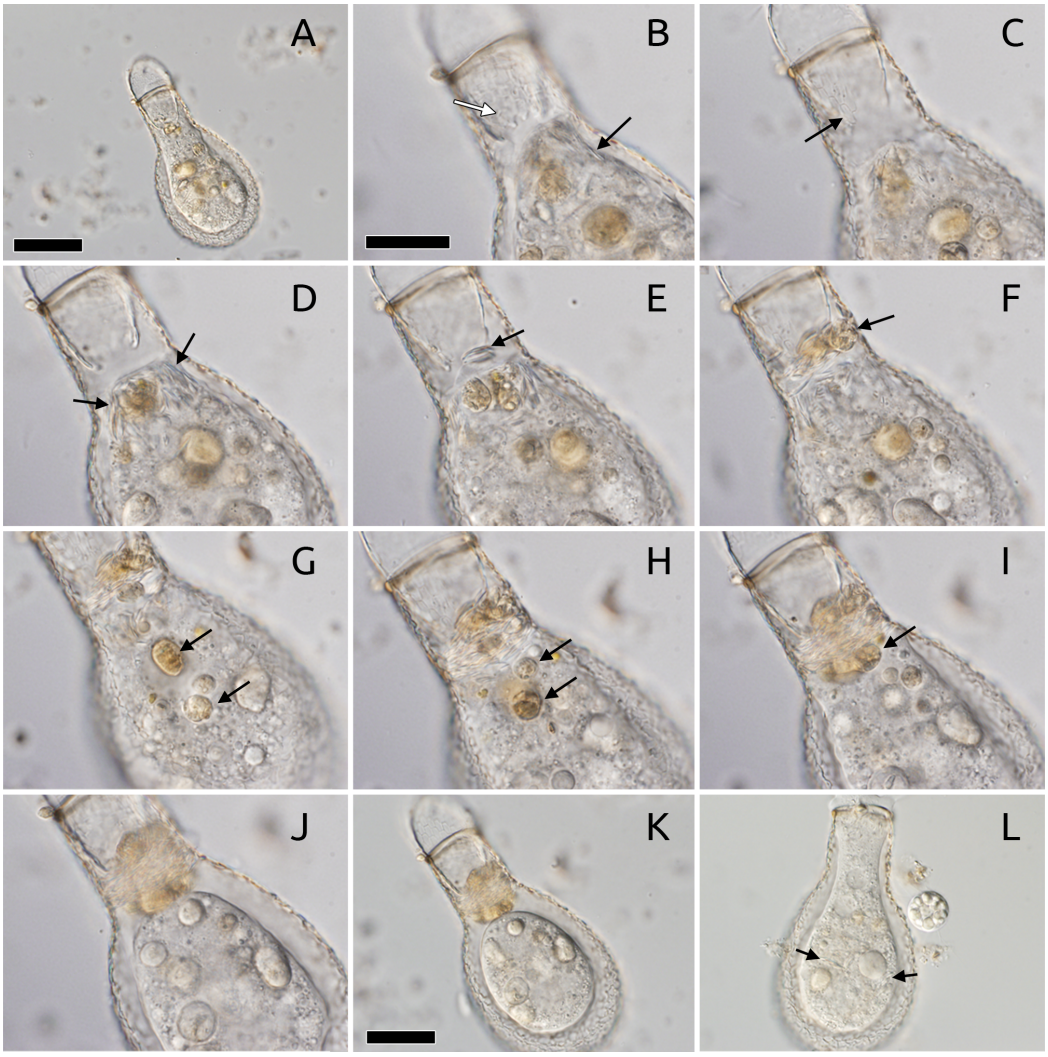

Figure 4 Kleptosquamy in *Padaungiella lageniformis*. (A) Lateral view of *P. lageniformis* ingesting cytoplasm of *Euglypha* sp., beginning of observations ($T = 0$). (B) View closer to the bottom of the plate, where the teardrop shaped apertural scales of the *Euglypha* individual are visible (white arrow), and other already ingested plates are in *P. lageniformis* cytoplasm (black arrow, $T = 22$ min). (C) A distinct optical section from B, showing a region in the *Euglypha* shell where the roughly hexagonal body plates (white arrow) were removed by the *P. lageniformis*, note that here the apertural scales are not present on this side ($T = 22$ min). (D) Accumulation of plates from *Euglypha* in the cytoplasmic region of *P. lageniformis* close to the aperture (black arrows), in the cytoplasm, plates are easily visible when in profile view ($T = 22$ min). (E) Early stage of apertural plug construction, the *P. lageniformis* has laid down two scales (black arrow) in a parallel orientation to the aperture ($T = 23$ min). (F) The organism begins to add other debris to the plug (black arrow, $t = 24$ min). (G) Debris particles had been added to the plug, notice vesicles of yellowish-brown material in the cytoplasm (black arrows), these are later added to the plug ($T = 1\ h$ 13 min). (H) Yellowish-brown debris moves closer to the aperture (black arrows, $T = 1$ h 13 min). (I) All debris particles finally added to the apertural plug (black arrows, $T = 1\ h$ 32 min). (J) After the apertural plug is finished, the cell goes into a cyst ($T = 1$ h 52 min). (K) Whole view of digestive cyst ($T = 1$ h 52 min). (L) Emergence of cyst 12 hours later, many scales are visible in the cytoplasm (black arrows), they were recollected from the plug. Other types of particles were discarded. Scale bar = 20 μm (B–J) and 50 μm (A, K, L).

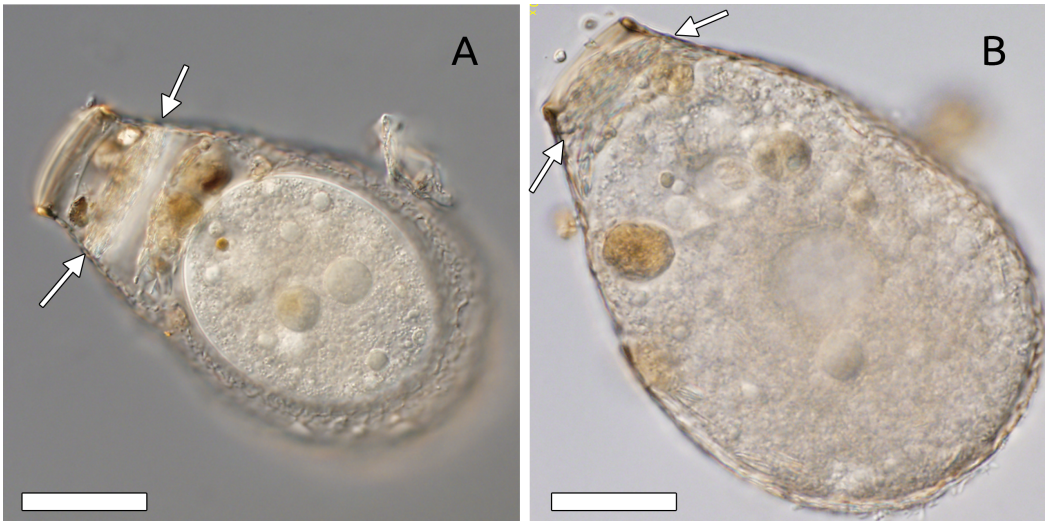

Figure 5 Evidence of kleptosquamy in other hyalosphenid genera. (A) A specimen of *Porosia bigibbosa* in a digestive cyst, with an apertural plug constructed partly with siliceous scales (white arrows). Specimen from mosses collected on an erratic boulder near the Merdasson river, Neuchâtel, Switzerland. (B) A specimen of *Nebela marginata*, about to enter the digestive cyst, presenting also an apertural plug constructed with a layer of siliceous scales (white arrows), among others. Specimen from *Sphagnum* collected in Les Pontins bog, Canton Bern, Switzerland. Scale bar = 50 µm.

Molecular clock reconstructions

To determine the origin of hyalosphenids, we generated a dated tree for the arcellinids (Fig. 7). In order to do so, we used the previously established opisthokont calibration points and a conservative calibration point for the minimum date of origin of the Arcellinida—this calibration point is used conservatively as calibrating the entire Arcellinida, as opposed to the less inclusive family Arcellidae as suggested by affinities in the original description (*Porter, Meisterfeld & Knoll, 2003*). In this reconstruction, we used the uncorrelated gamma multipliers model for the distribution of divergence times. This is because in our model fit analyses, this model yielded the largest Bayes Factor (logBF interval of 18.7–26.9, against 12.8–14.5 for CIR model and 16.6–24.7 for lognormal model). The Bayes Factor is one of many proposed methods to measure the appropriateness of a given model for the data at hand, and a larger BF indicates a better model fit (*Lartillot & Philippe, 2006*). Hence, all results discussed are based on that model. The reconstruction ran for circa 55,000 cycles until convergence between the two chains was achieved.

Our reconstruction stands in sharp contrast with another recent molecular clock reconstruction of the arcellinids (*Fiz-Palacios, Leander & Heger, 2014*). The two most likely reasons for this are: (1) although Fiz-Palacios and colleagues used a part of the same dataset used here, we focused on the SSU rDNA partition and not on the protein coding partition; (2) we included mostly opisthokont fossils as calibration points, but Fiz-Palacios and colleagues used a number of Meso- and Cenozoic microfossils as calibration points for internal families of arcellinids. To test the influence of these hypotheses, we implemented the calibration points suggested by Fiz-Palacios in our framework. This yielded an

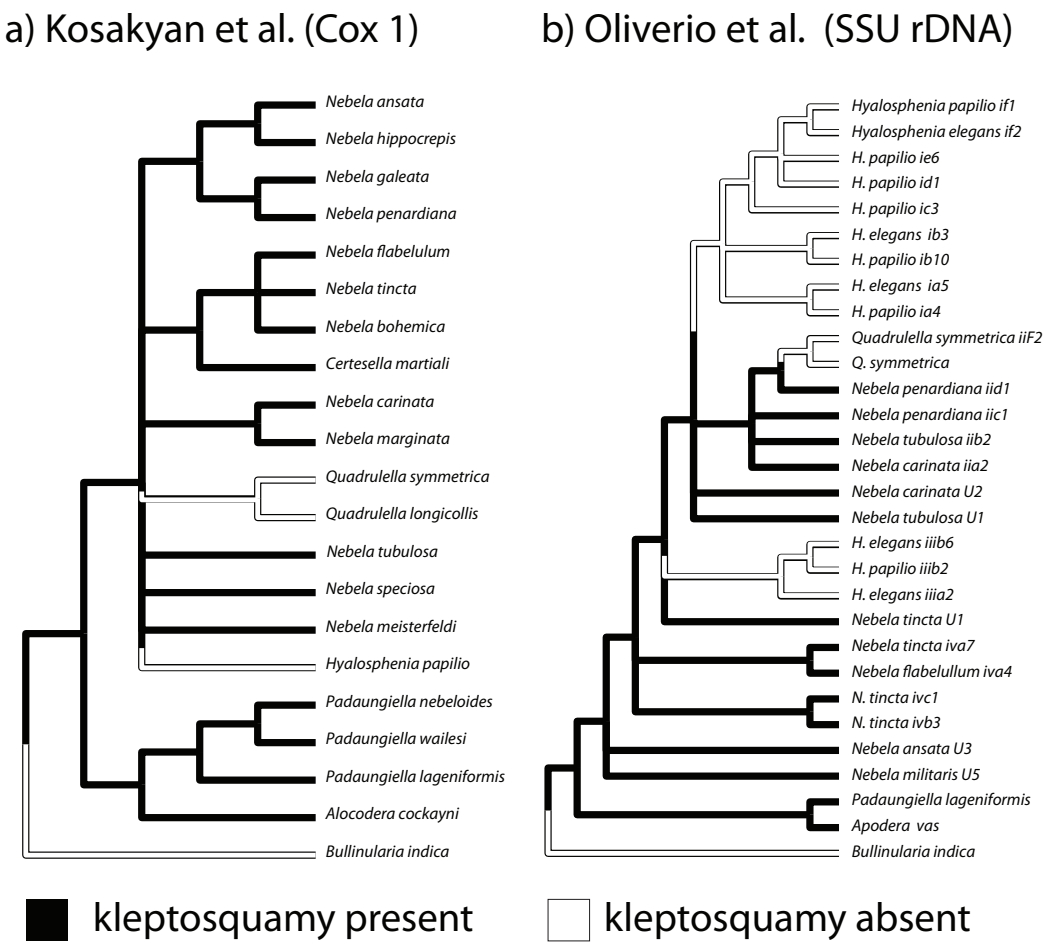

Figure 6 Ancestral state reconstruction of kleptosquamy in the hyalosphenid genera. The backbone of each cladogram is one of two most current hyalosphenid phylogenies, based on distinct sets of genes. Colors along the tree branches represent how states changed through evolution for this character.

additional tree (Fig. 7, right). This tree is very similar to the tree obtained by Fiz-Palacios and colleagues, with all origins of groups tending to appear at younger dates. For instance, the origin of arcellinids as a whole shifts from 944 mya to 600 mya using the Meso- and Cenozoic fossils. This is representative of a general trend throughout the tree. Therefore, the distinct dates obtained in the reconstruction presented in Fig. 7 probably do not stem from focusing on the SSU rDNA partition, but rather from the use of distinct calibration points. Hence, the interpretation of fossils is paramount in defining which result is more likely to reconstruct the actual history of Arcellinida.

DISCUSSION

Kleptosquamy can be inferred as an ancestral character state in hyalosphenids (Fig. 6), i.e., the last common ancestor of all extant hyalosphenids was able to re-use euglyphid scales. Hyalosphenid biology is not well understood, because most attempts to culture these organisms have failed. Strains that have been maintained for a certain time (*Nebela collaris*) had to be fed with fast-growing species of euglyphids, such as *Euglypha hyalina*

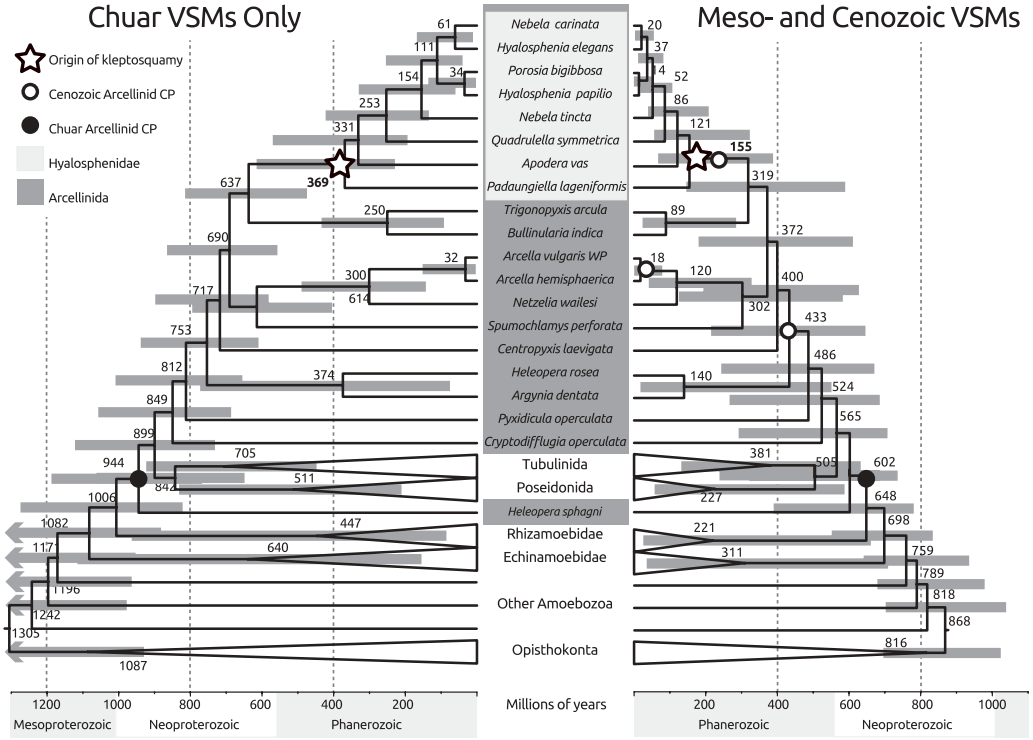

Figure 7 Comparison between dated phylogenies of Arcellinida based on molecular clock reconstructions using distinct sets of calibration points. Both reconstructions were based on a 109 taxon, 914 positions alignment. Taxa that are not relevant for the present discussion have been collapsed for clarity. The reconstruction on the left uses a single arcellinid calibration point (indicated), and other 5 calibration points inside the Opisthokonta. The reconstruction on the right uses the previous 6 calibration points plus 3 additional arcellinid calibration points. Although the mean value for node times can be quite different, both reconstructions are within the 95% confidence interval of each other (indicated by shaded horizontal bars).

(Meisterfeld, pers. comm., 2013). For instance, one cannot say with certainty whether a hyalosphenid is able to construct the shell without any euglyphid scales. This caveat undermines the interpretation of klepstosquamy as ancestral in the group, for this reason, we clearly establish that our *working* hypothesis is that scaled euglyphids appeared before hyalosphenids.

The fossil record of euglyphids is quite sparse and does not currently allow accurate timing of their evolution. The very well documented microfossils of *Scutiglypha* from diatomaceous earth demonstrate that modern genera have existed for at least 15 million years (*Foissner & Schiller, 2001*). More recently, Eocene microfossils have unambiguously pushed the fossil record of euglyphids back to 50 million years ago (*Barber, Siver & Karis, 2013*), including members of the genus *Scutiglypha* (Euglyphidae). Older records of shells are much more difficult to interpret, as the conditions of shell preservation make the separation between arcellinids and euglyphids ever more difficult: because of intense convergence, pseudopods would be the only reliable way of separating arcellinids and euglyphids, but these are usually not preserved in the fossil record (*Bosak et al., 2011*; *Lahr et al., 2014*). For instance, some vase shaped microfossils described from the

Chuar group, especially *Melicerion poikilon*, *Bonniea* spp. and *Bombycion micron* have morphological characteristics that are compatible with euglyphid testate amoebae: the typical vase shape, thin walls, terminal aperture, homogeneously shaped and sized scales and an apparent siliceous composition. However, an arcellinid origin cannot be excluded, *Quadrulella*, a modern arcellinid, shares all those features (*Porter & Knoll, 2000*; *Porter, Meisterfeld & Knoll, 2003*). Hence, new discoveries of exceptionally preserved and properly described arcellinid and euglyphid fossils are necessary to inform interpretations of origin and diversification (*Bosak et al., 2011*; *Dalton et al., 2013*; *Fiz-Palacios, Leander & Heger, 2014*; *Strauss et al., 2014*).

The dated reconstruction presented here uses a single-locus and external calibration points to the arcellinids and places the origin of hyalosphenids in the Paleozoic (about 370 mya, with a 95% confidence interval that extends from the Neoproterozoic to Triassic). This is in marked contrast to the recent reconstruction of arcellinid history by *Fiz-Palacios, Leander & Heger (2014)*, which placed the origin of hyalosphenids in the Cretaceous, about 130 mya (with a 95% confidence interval between the Devonian and the Eocene). These authors used a very similar dataset, but included both the SSU rDNA and five additional protein coding genes (both analyses are based on the dataset published by *Lahr, Grant & Katz, 2013*). The 240 million year difference between the two reconstructions is significant and may lead to very distinct implications. The use of the same calibration points as Fiz-Palacios and colleagues, combined with our search strategy, produced a tree that is very similar to the results of Fiz-Palacios et al. and estimate a Cretaceous rise of hyalospheniids. The additional calibration points used are controversial, some are based on fossils whose descriptions have not clearly established syngenicity with the matrix and may be contaminants (*Farooqui et al., 2010*; *Kumar, 2011*); others come from amber and the identity of organisms is established using optical microscopy alone (*Schmidt, Schönborn & Schäfer, 2004*; *Schmidt et al., 2006*; *Girard et al., 2011*). The inclusion of these fossils as calibration points led to an interesting scenario interpreted by *Fiz-Palacios, Leander & Heger (2014)*: that hyalosphenids are an ancient lineage that diversified when the complex peatland environments became available. The caveat is that many aspects of the identities of fossils used as calibration points remain to be clarified—this does not mean that the interpretations are incorrect.

The new molecular clock reconstruction (Fig. 7) suggests that various testate amoebae including hyalospheniids, the aquatic *Arcella* + *Netzelia* clade, as well as the soil dwelling *Trigonopyxis* + *Bullinularia* clade have diversified after the mid-Devonian. In contrast to the preceding periods, when plant cover was restricted to moist habitats, the Late Devonian and the Carboniferous saw the diversification of plants that were well adapted to life on land, with deeper roots and soil forming capabilities (e.g., *Gibling & Davies, 2012*; *Kenrick et al., 2012*). These plants formed extensive forests, established their own, humid environments, and produced abundant organic matter as well as soils (*Kenrick et al., 2012*), matching the appearance of the *Bullinularia* clade. These evolutionary events likely influenced the Si cycling on land as well due to two main factors: (1) The root systems of the Late Devonian/Carboniferous plants are thought to have promoted silicate weathering

(e.g., *Algeo, Scheckler & Maynard, 2001*), and (2) tree-like Lycopodiophyta, Equisetales and liverworts, plants whose modern relatives can accumulate as much or more Si than grasses (*Hodson et al., 2005*), were abundant in forest ecosystems. Our new molecular clock reconstruction and the coinciding sequence of evolutionary and ecological changes that have been documented in the fossil record inspire questions. Did the release of Si from plants and the accumulation of Si in the plates of biomineralizing testate amoebae as well as in various predatory species strengthen the links between the C and the Si cycles on land? The annual rate of biosilification by testate amoebae was shown to be of the same order as the uptake rate by trees (*Aoki, Hoshino & Matsubara, 2007*; *Sommer et al., 2012*; *Puppe et al., 2014*) and the size of the Si pool in testate amoebae increases with vegetation development in some early ecosystem successions (*Puppe et al., 2014*).

To move forward from here, we need to (i) better understand Si metabolism across protist groups, including deeper understanding of physiological aspects; (ii) obtain reliable fossil evidence for the appearance and diversification of Si-metabolizing lineages; (iii) improve the molecular clock by expanding the molecular database, using appropriate numerical models and carefully checking the reliability of the fossil record, (iv) improve constraints on the contribution of Si-precipitating organisms to the cycling of Si and C in terrestrial systems. The combination of these efforts is challenging, but can be met with a combination of approaches including molecular phylogeny, biogeochemistry, and paleontology.

ACKNOWLEDGEMENTS

We thank Piet-Louis Grundling for collecting the *Sphagnum* sample from which the *Quadrulella* illustrated in Fig. 2A was found. We also thank the associate editor as well as two reviewers for relevant criticism of the manuscript.

ADDITIONAL INFORMATION AND DECLARATIONS

Funding

The digitalization of Eugene Pénard's slide collection was made possible by a Wikimedia.ch fund. DJGL is funded by a FAPESP Young Investigator Award (2013/04585-3); TB is funded by NASA Astrobiology Institute award NNA13AA90A and NASA Exobiology award 6927184. Traveling was partly funded by a CNPq-MIT seed fund (#551952/2011-3) to DJGL and TB. Sampling and microscopic analyses were funded by a "fonds de donation" from the University of Neuchatel through a post-doctoral fellowship to DJGL in collaboration with EADM and EL. The funders had no role in study design, data collection and analysis, decision to publish, or preparation of the manuscript.

Grant Disclosures

The following grant information was disclosed by the authors:
Wikimedia.ch fund.
FAPESP Young Investigator Award: 2013/04585-3.
NASA Astrobiology Institute award: NNA13AA90A.

NASA Exobiology award: 6927184.
CNPq-MIT seed fund: #551952/2011-3.
University of Neuchatel.

Competing Interests

The authors declare there are no competing interests.

Author Contributions

- Daniel J.G. Lahr conceived and designed the experiments, performed the experiments, analyzed the data, contributed reagents/materials/analysis tools, wrote the paper, prepared figures and/or tables, reviewed drafts of the paper.
- Tanja Bosak analyzed the data, contributed reagents/materials/analysis tools, wrote the paper, reviewed drafts of the paper.
- Enrique Lara analyzed the data, wrote the paper, reviewed drafts of the paper.
- Edward A.D. Mitchell conceived and designed the experiments, analyzed the data, contributed reagents/materials/analysis tools, wrote the paper, reviewed drafts of the paper.

Data Availability

The following information was supplied regarding data availability:

The alignments and trees used, as well as a document with instructions and command lines used for running analyses, are available as a supplemental file.

Supplemental Information

Supplemental information for this article can be found online at http://dx.doi.org/10.7717/peerj.1234#supplemental-information.

REFERENCES

Alexandre A, Meunier J-D, Colin F, Koud J-M. 1997. Plant impact on the biogeochemical cycle of silicon and related weathering processes. *Geochimica et Cosmochimica Acta* **61**:677–682 DOI 10.1016/S0016-7037(97)00001-X.

Algeo TJ, Scheckler SE, Maynard JB. 2001. Effects of the middle to Late Devonian spread of vascular land plants on weathering regimes, marine biotas, and global climate. In: Gensel PG, Edwards D, eds. *Plants invade the land: evolutionary and environmental perspectives.* New York: Columbia University Press, 213–236.

Anderson OR. 1987. Fine structure of a silica-biomineralizing testate amoeba, *Netzelia tuberculata*. *The Journal of Protozoology* **34**:302–309 DOI 10.1111/j.1550-7408.1987.tb03180.x.

Anderson OR. 1989. Some observations of feeding behavior, growth, and test particle morphology of a silica-secreting testate amoeba *Netzelia tuberculata* (Wallich) (Rhizopoda, Testacea) grown in laboratory culture. *Archiv für Protistenkunde* **137**:211–221 DOI 10.1016/S0003-9365(89)80027-2.

Anderson OR. 1994. Cytoplasmic origin and surface deposition of siliceous structures in Sarcodina. *Protoplasma* **181**:61–77 DOI 10.1007/BF01666389.

Aoki Y, Hoshino M, Matsubara T. 2007. Silica and testate amoebae in a soil under pine–oak forest. *Geoderma* **142**:29–35 DOI 10.1016/j.geoderma.2007.07.009.

Barber A, Siver PA, Karis W. 2013. Euglyphid testate amoebae (Rhizaria: Euglyphida) from an arctic eocene waterbody: evidence of evolutionary stasis in plate morphology for over 40 million years. *Protist* **164**:541–555 DOI 10.1016/j.protis.2013.05.001.

Benton MJ, Donoghue PC, Asher RJ, Friedman M, Near TJ, Vinther J. 2015. Constraints on the timescale of animal evolutionary history. *Palaeontologia Electronica* **18**:1–106.

Bosak T, Lahr DJG, Pruss SB, Macdonald FA, Dalton L, Matys E. 2011. Agglutinated tests in post-Sturtian cap carbonates of Namibia and Mongolia. *Earth and Planetary Science Letters* **308**:29–40 DOI 10.1016/j.epsl.2011.05.030.

Cary L, Alexandre A, Meunier J-D, Boeglin J-L, Braun J-J. 2005. Contribution of phytoliths to the suspended load of biogenic silica in the Nyong basin rivers (Cameroon). *Biogeochemistry* **74**:101–114 DOI 10.1007/s10533-004-2945-1.

Châtelet EAdu, Noiriel C, Delaine M. 2013. Three-dimensional morphological and mineralogical characterization of testate amebae. *Microscopy and Microanalysis* **19**:1511–1522 DOI 10.1017/S1431927613013226.

Conley DJ. 2002. Terrestrial ecosystems and the global biogeochemical silica cycle. *Global Biogeochemical Cycles* **16**:68-1–68-8 DOI 10.1029/2002GB001894.

Cornelis J-T, Delvaux B, Georg RB, Lucas Y, Ranger J, Opfergelt S. 2011. Tracing the origin of dissolved silicon transferred from various soil-plant systems towards rivers: a review. *Biogeosciences* **8**:89–112 DOI 10.5194/bg-8-89-2011.

Dalton LA, Bosak T, Macdonald FA, Lahr DJG, Pruss SB. 2013. Preservational and morphological variability of assemblages of agglutinated eukaryotes in cryogenian cap carbonates of northern Namibia. *PALAIOS* **28**:67–79 DOI 10.2110/palo.2012.p12-084r.

Deflandre G. 1936. Etude monographique sur le genre *Nebela* Leidy. *Annales de Protistologie* **5**:201–286.

Donoghue PC, Benton MJ. 2007. Rocks and clocks: calibrating the Tree of Life using fossils and molecules. *Trends in Ecology & Evolution* **22**:424–431 DOI 10.1016/j.tree.2007.05.005.

Douglas MSV, Smol JP. 2001. Siliceous protozoan plates and scales. In: Smol JP, Birks HJB, Last WM, Bradley RS, Alverson K, eds. *Tracking environmental change using lake sediments, Developments in paleoenvironmental research.* Netherlands: Springer, 265–279.

Farooqui A, Kumar A, Jha N, Pande AC, Bhattacharya DD. 2010. A thecamoebian assemblage from the Manjir formation (early Permian) of northwest Himalaya, India. *E-Journal Earth Science India* **3**:146–153.

Fiz-Palacios O, Leander BS, Heger TJ. 2014. Old lineages in a new ecosystem: diversification of arcellinid amoebae (Amoebozoa) and peatland mosses. *PLoS ONE* **9**:e95238 DOI 10.1371/journal.pone.0095238.

Foissner W, Schiller W. 2001. Stable for 15 million years: scanning electron microscope investigation of Miocene euglyphid thecamoebians from Germany, with description of the new genus *Scutiglypha*. *European Journal of Protistology* **37**:167–180 DOI 10.1078/0932-4739-00012.

Gibling MR, Davies NS. 2012. Palaeozoic landscapes shaped by plant evolution. *Nature Geoscience* **5**:99–105 DOI 10.1038/ngeo1376.

Girard V, Néraudeau D, Adl SM, Breton G. 2011. Protist-like inclusions in amber, as evidenced by Charentes amber. *European Journal of Protistology* **47**:59–66 DOI 10.1016/j.ejop.2010.12.003.

Gomaa F, Todorov M, Heger TJ, Mitchell EAD, Lara E. 2012. SSU rRNA phylogeny of Arcellinida (Amoebozoa) reveals that the largest Arcellinid genus, *Difflugia* Leclerc 1815, is not Monophyletic. *Protist* **163**:389–399 DOI 10.1016/j.protis.2011.12.001.

Gröger C, Lutz K, Brunner E. 2008. Biomolecular self-assembly and its relevance in silica biomineralization. *Cell Biochemistry and Biophysics* **50**:23–39 DOI 10.1007/s12013-007-9003-2.

Hedley DRH, Ogden CG. 1974. Adhesion plaques associated with the production of a daughter cell in *Euglypha* (Testacea; Potozoa). *Cell and Tissue Research* **153**:261–268 DOI 10.1007/BF00226614.

Heger TJ, Pawlowski J, Lara E, Leander BS, Todorov M, Golemansky V, Mitchell EAD. 2011. Comparing potential COI and SSU rDNA barcodes for assessing the diversity and phylogenetic relationships of cyphoderiid testate amoebae (Rhizaria: Euglyphida). *Protist* **162**:131–141 DOI 10.1016/j.protis.2010.05.002.

Hodson MJ, White PJ, Mead A, Broadley MR. 2005. Phylogenetic variation in the silicon composition of plants. *Annals of Botany* **96**:1027–1046 DOI 10.1093/aob/mci255.

Karlstrom KE, Bowring SA, Dehler CM, Knoll AH, Porter SM, Des Marais DJ, Weil AB, Sharp ZD, Geissman JW, Elrick MB, Timmons JM, Crossey LJ, Davidek KL. 2000. Chuar group of the Grand Canyon: record of breakup of Rodinia, associated change in the global carbon cycle, and ecosystem expansion by 740 Ma. *Geology* **28**:619–622 DOI 10.1130/0091-7613(2000)28<619:CGOTGC>2.0.CO;2.

Katz LA. 2012. Origin and diversification of eukaryotes. *Annual Review of Microbiology* **66**:411–427 DOI 10.1146/annurev-micro-090110-102808.

Kenrick P, Wellman CH, Schneider H, Edgecombe GD. 2012. A timeline for terrestrialization: consequences for the carbon cycle in the Palaeozoic. *Philosophical Transactions of the Royal Society of London B: Biological Sciences* **367**:519–536 DOI 10.1098/rstb.2011.0271.

Kosakyan A, Heger TJ, Leander BS, Todorov M, Mitchell EAD, Lara E. 2012. COI barcoding of nebelid testate amoebae (Amoebozoa: Arcellinida): extensive cryptic diversity and redefinition of the Hyalospheniidae schultze. *Protist* **163**:415–434 DOI 10.1016/j.protis.2011.10.003.

Kumar A. 2011. Acid-resistant Cretaceous thecamoebian tests from the Arabian Peninsula: a suggestion for study of agglutinated rhizopods in palynological slides. *Journal of Micropalaeontology* **30**:1–5 DOI 10.1144/0262-821X10-018.

Lahr DJG, Grant JR, Katz LA. 2013. Multigene phylogenetic reconstruction of the tubulinea (amoebozoa) corroborates four of the six major lineages, while additionally revealing that shell composition does not predict phylogeny in the Arcellinida. *Protist* **164**:323–339 DOI 10.1016/j.protis.2013.02.003.

Lahr DJ, Laughinghouse HD, Oliverio AM, Gao F, Katz LA. 2014. How discordant morphological and molecular evolution among microorganisms can revise our notions of biodiversity on earth. *BioEssays* **36**:950–959 DOI 10.1002/bies.201400056.

Lara E, Heger TJ, Ekelund F, Lamentowicz M, Mitchell EAD. 2008. Ribosomal RNA genes challenge the monophyly of the Hyalospheniidae (Amoebozoa: Arcellinida). *Protist* **159**:165–176 DOI 10.1016/j.protis.2007.09.003.

Lartillot N, Lepage T, Blanquart S. 2009. PhyloBayes 3: a Bayesian software package for phylogenetic reconstruction and molecular dating. *Bioinformatics* **25**:2286–2288 DOI 10.1093/bioinformatics/btp368.

Lartillot N, Philippe H. 2006. Computing bayes factors using thermodynamic integration. *Systematic Biology* **55**:195–207 DOI 10.1080/10635150500433722.

Leidy J. 1879. *Fresh-water rhizopods of North America*. Washington, D.C.: Government Printing Office.

Maddison WP, Maddison DR. 2011. *Mesquite: a modular system for evolutionary analysis*. Version 2.75. *Available at http://mesquiteproject.org*.

Marron AO, Alston MJ, Heavens D, Akam M, Caccamo M, Holland PWH, Walker G. 2013. A family of diatom-like silicon transporters in the siliceous loricate choanoflagellates. *Proceedings of the Royal Society B: Biological Sciences* **280**:20122543 DOI 10.1098/rspb.2012.2543.

Meisterfeld R. 2002. Order Arcellinida Kent, 1880. *The Illustrated Guide to the Protozoa* **2**:827–860.

Oliverio AM, Lahr DJG, Nguyen T, Katz LA. 2014. Cryptic diversity within morphospecies of testate amoebae (Amoebozoa: Arcellinida) in new England bogs and fens. *Protist* **165**:196–207 DOI 10.1016/j.protis.2014.02.001.

Parfrey LW, Lahr DJG, Knoll AH, Katz LA. 2011. Estimating the timing of early eukaryotic diversification with multigene molecular clocks. *Proceedings of the National Academy of Sciences of the United States of America* **108**:13624–13629 DOI 10.1073/pnas.1110633108.

Penard E. 1902. *Faune rhizopodique du bassin du Léman*. Genève: H. Kündig.

Porter SM, Knoll AH. 2000. Testate amoebae in the Neoproterozoic Era: evidence from vase-shaped microfossils in the Chuar group, Grand Canyon. *Paleobiology* **26**:360–385 DOI 10.1666/0094-8373(2000)026<0360:TAITNE>2.0.CO;2.

Porter SM, Meisterfeld R, Knoll AH. 2003. Vase-shaped microfossils from the Neoproterozoic Chuar group, Grand Canyon: a classification guided by modern testate amoebae. *Journal of Paleontology* **77**:409–429 DOI 10.1666/0022-3360(2003)077<0409:VMFTNC>2.0.CO;2.

Puppe D, Kaczorek D, Wanner M, Sommer M. 2014. Dynamics and drivers of the protozoic Si pool along a 10-year chronosequence of initial ecosystem states. *Ecological Engineering* **70**:477–482 DOI 10.1016/j.ecoleng.2014.06.011.

Rutschmann F. 2005. *Bayesian molecular dating using PAML/multidivtime. A step-by-step manual*. Switzerland: University of Zurich. *Available at http://www.plant.ch*.

Sapriel G, Quinet M, Heijde M, Jourdren L, Tanty V, Luo G, Le Crom S, Lopez PJ. 2009. Genome-wide transcriptome analyses of silicon metabolism in *phaeodactylum tricornutum* reveal the multilevel regulation of silicic acid transporters. *PLoS ONE* **4**:e7458 DOI 10.1371/journal.pone.0007458.

Sarmiento JL. 2013. *Ocean biogeochemical dynamics*. Princeton University Press, 528 pp.

Schmidt AR, Ragazzi E, Coppellotti O, Roghi G. 2006. A microworld in Triassic amber. *Nature* **444**:835 DOI 10.1038/444835a.

Schmidt AR, Schönborn W, Schäfer U. 2004. Diverse fossil amoebae in German Mesozoic amber. *Palaeontology* **47**:185–197 DOI 10.1111/j.0031-0239.2004.00368.x.

Sommer M, Jochheim H, Höhn A, Breuer J, Zagorski Z, Busse J, Barkusky D, Puppe D, Wanner M, Kaczorek D. 2012. Si cycling in a forest biogeosystem—the importance of anthropogenic perturbation and induced transient state of biogenic Si pools. *Biogeosciences Discussions* **9**:18865–18906 DOI 10.5194/bgd-9-18865-2012.

Strauss JV, Rooney AD, Macdonald FA, Brandon AD, Knoll AH. 2014. 740 Ma vase-shaped microfossils from Yukon, Canada: implications for Neoproterozoic chronology and biostratigraphy. *Geology* G35736.1.

Thorne JL, Kishino H. 2003. Multidivtime. *Available at http://statgen.ncsu.edu/thorne/multidivtime.html*.

Vucetich MC. 1974. Comentarios criticos sobre *Argynnia* Jung, 1942 (Rhizopoda, Testacea). *Neotropica* **20**:126–128.

Wilkinson DM. 2008. Testate amoebae and nutrient cycling: peering into the black box of soil ecology. *Trends in Ecology & Evolution* **23**:596–599 DOI 10.1016/j.tree.2008.07.006.

Wilkinson DM, Mitchell EAD. 2010. Testate amoebae and nutrient cycling with particular reference to soils. *Geomicrobiology Journal* **27**:520–533 DOI 10.1080/01490451003702925.

Yang Z. 2007. PAML 4: phylogenetic analysis by maximum likelihood. *Molecular Biology and Evolution* **24**:1586–1591 DOI 10.1093/molbev/msm088.